Global distribution changes in coccolithophore blooms

E. K. Duncan[1,2], D. Clewley[1], T. Smyth[1,3*]

[1]Plymouth Marine Laboratory, Prospect Place, Plymouth, PL1 3DH, United Kingdom.

[2]University of Exeter, Stocker Road, Exeter, EX4 4PY

[3]Centre for Geography and Environmental Science, Department of Earth and Environmental Sciences, University of Exeter, Penryn Campus, Penryn, Cornwall, TR10 9EZ

*Corresponding author: Tim Smyth (tjsm@pml.ac.uk)

Key Points:

- Marked changes in global ocean coccolithophore bloom distribution over the past 40 years.
- Overall global decrease in bloom area of 1.15 million km^2.
- Increased occurrence in Barents Sea, Antarctic Ocean and East Africa coastal province driven primarily by changes in sea-surface temperature.
- Decreased occurrence elsewhere, driven by multiple factors in different provinces, elucidated using Machine Learning.

Abstract

The global distribution of high Remote-sensing reflectance (Rrs) waters visible from satellite, likely associated with coccolithophore blooms, has changed markedly over the past 40 years. Over that period there has globally been an overall decrease in bloom area of 1.15 million km^2 but with notable Rrs increases in the Barents Sea and the Antarctic Ocean. The primary drivers of these fundamental changes to ocean biogeochemistry have been investigated using Machine Learning techniques together with contemporaneous global multi-decadal time-series of sea-surface temperature (SST); wind speed and stress; sea level anomaly (SLA); photosynthetically available radiation (PAR) and; mixed layer depth (MLD). When split into ocean provinces different drivers of positive and negative trends in Rrs were found to dominate in different regions, but generally increases were found to coincide with changes to SST, PAR and reductions to wind-speed.

Plain Language Summary

Coccolithophore blooms are sensitive to changes in ocean climate and we show a global reduction in their occurrence over the past 40 years. However, more intense blooms are likely happening in high latitude regions such as the Barents Sea and Antarctic Ocean, driven by changes in sea temperature, levels of sunlight and reductions in ocean wind-mixing.

1 Introduction

Coccolithophores are a group of marine phytoplankton that synthesise external calcium carbonate platelets (coccoliths) and play a critical role in the global carbon cycle [*Rost and Riebesell*, 2004] and marine biogeochemistry [*Balch*, 2018]. During the latter stages of a bloom the coccoliths are shed in large numbers giving the water a turquoise-white appearance which is readily detectable at the surface [*Smyth et al.*, 2002; *Tyrrell et al.*, 1999] and from space [*Gordon et al.*, 2001]. It is this unique satellite visibility, which is not available for any other phytoplankton species, which enables examination of temporal changes in their global distribution [*Brown and Yoder*, 1994; *Iglesias-Rodriguez et al.*, 2002; *Loveday and Smyth*, 2018; *Winter et al.*, 2013] and any associated large scale drivers. Previous regionally focused work has shown coccolithophores to be advancing into some sub-polar seas (Barents - [*Smyth et al.*, 2004]; Bering - [*Merico et al.*, 2003]; Southern Ocean - *Balch et al.* [2016]) while perhaps becoming more scarce in some (Gulf of Maine - [*Balch et al.*, 1991]), but not all (Bay of Biscay - [*Morozov et al.*, 2013]), parts of their mid-latitude distribution. Coccolithophores may therefore be sensitive to, and important indicators of, environmental change.

In this paper, the changes in global coccolithophore bloom distribution are examined over a 40 year time period using the consistently calibrated Remote-sensing reflectance (Rrs) dataset [*Loveday and Smyth*, 2018] derived from the visible-channel Advanced Very-High Resolution Radiometer (AVHRR) PATMOS-x [*Heidinger et al.*, 2010] climate data record. Despite lower technical specifications rendering AVHRR only 11 % as sensitive to variations in coccolithophore visible reflectance compared with ocean colour channels [*Groom and Holligan*, 1987] higher Rrs associated with coccolithophore blooms and corroborated by independent sources [*Loveday and Smyth*, 2018] are clearly apparent in the dataset. Long-term multi-decadal, fine-scale ($< 1°$) global datasets are used together with the primary Rrs dataset, within a Machine Learning framework, to determine the drivers of coccolithophore bloom shifts in occurrence. By integrating these different data sources within such a framework, covering a

sufficiently long (40 year) time-period [*Henson et al.*, 2009], this study sheds new light on the drivers of global coccolithophore bloom distribution which in turn may have consequences for the Earth system carbon cycle.

2 Data and Methods

The primary dataset used was the consistently calibrated 40-year timeseries of visible channel Rrs from the AVHRR satellite sensor [*Loveday and Smyth*, 2018]. Initial investigations showed high Rrs in the Southern Ocean to be strongly correlated with sea ice fraction. To minimize signal contamination, Rrs was masked by the European Space Agency (ESA) Climate Change Initiative (CCI) Sea Surface Temperature (SST) daily sea ice extent product [*Merchant et al.*, 2014]. This daily product was averaged to monthly and remapped using bilinear interpolation from 0.05° to 0.1° in order to match the Rrs dataset spatio-temporal resolution. The resulting refined version of the global Rrs dataset [*Loveday and Smyth*, 2018] is shown in Figure 1.

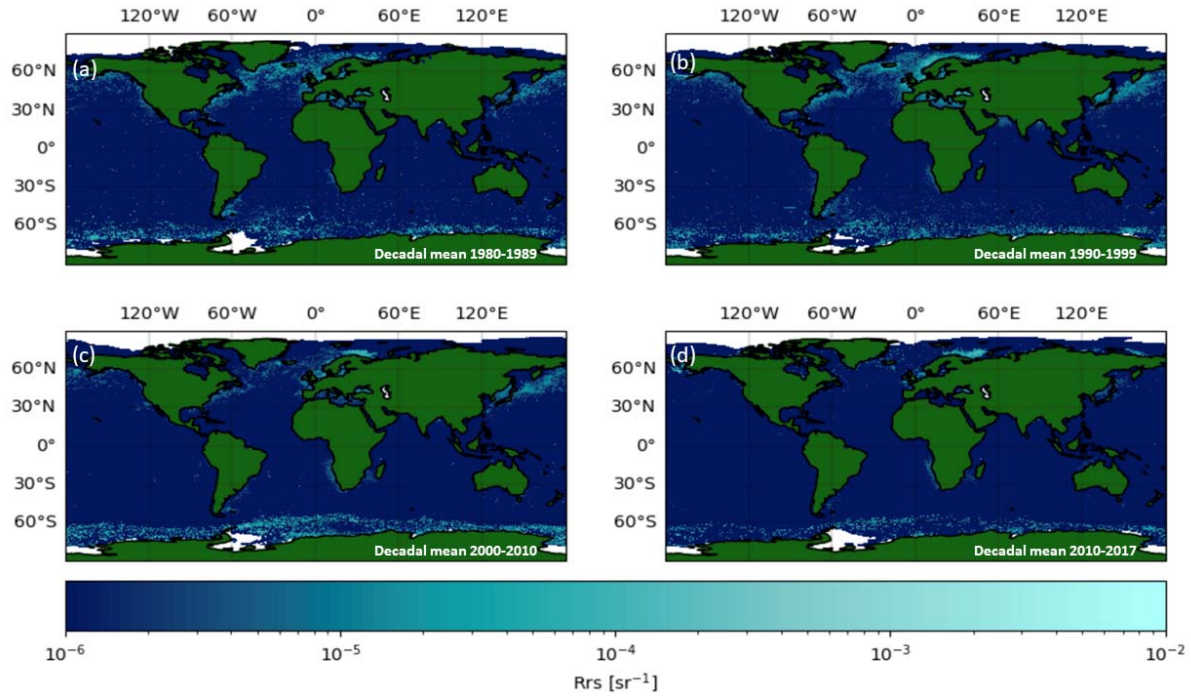

Figure 1. Decadal mean Rrs with associated ice mask shown in white: a) 1980 - 1989; b) 1990 - 1999; c) 2000 - 2009; d) 2010 – 2017.

To enable investigation of the key drivers of coccolithophore bloom distribution, temporal overlap of potentially relevant global meteorological and oceanographic timeseries and the primary Rrs dataset were maximized (Table 1). The altimeter satellite gridded sea level anomaly (SLA) is pre-computed with respect to a 20-year mean (1993-2012). The wind speed and stress were obtained at a 6h time resolution in order to compute monthly mean and standard deviation thereby providing a measure of variability. For the data products which have a lower spatial resolution than the Rrs dataset (Wind, SLA, PAR, MLD), a nearest neighbour approach was used to remap to a 0.1° grid.

Table 1. Input global datasets and their provenance used in this study showing timespan, temporal and spatial resolution.

Variable	Dataset	Spatial resolution (degrees)	Native temporal resolution	Start date – End date	Source reference
Remote Sensing Reflectance (Rrs)	AVHRR	0.10° × 0.10°	Monthly	01/01/1979 – 01/01/2018	10.1594/PANGAEA.892175
Sea ice extent	ESA SST_cci	0.05° × 0.05°	Daily	01/09/1981 - 01/12/2016	10.48670/moi-00185
Sea surface temperature (SST)	ESA SST_cci	0.05° × 0.05°	Daily	01/09/1981 - 01/12/2016	10.48670/moi-00185
Sea level anomaly (SLA)	SEALEVEL_GLO	0.25° × 0.25°	Monthly	01/01/1993 - 01/12/2016	10.48670/moi-00148
Wind speed and stress[1]	IFREMER CERSAT	0.25° × 0.25°	6 hourly	01/01/1992 - 01/01/2020	10.48670/moi-00185
Photosynthetically Available Radiation (PAR)	ECMWF ERA-Interim	0.85° × 0.85°	Monthly mean of daily accumulation	01/01/1982 - Present	*Simmons et al.* [2006] 10.21957/pocnex23c6
Mixed layer depth (MLD)	ECMWF ERA-Interim	0.85° × 0.85°	Monthly	01/01/1980 - 01/01/2014	*Simmons et al.* [2006] 10.21957/pocnex23c6

2.1 Trend analysis

In order to capture identify key global trends and drivers of coccolithophore blooms, the datasets (Table 1) were partitioned into the ecological provinces defined in *Longhurst* [1998]. In this approach we assume homogeneity regarding the drivers and trends in Rrs across each province, with the exception of the Atlantic subarctic province. Here an initial analysis per Rrs grid point demonstrated the Norwegian Sea to have very strong negative trend, and the Barents Sea a very positive trend. Therefore, this province was split in two for analysis.

[1] WIND_GLO_WIND_L4_REP_OBSERVATIONS_012_006 product replaced by WIND_GLO_PHY_L4_MY_012_006 in March 2023, E.U Copernicus Marine Service Information (CMEMS), Marine Data Store (MDS).

The trend analysis was conducted on the 12-month rolling mean (to de-seasonalise) of the Rrs timeseries. A Mann-Kendal [*Kendall*, 1975; *Mann*, 1945] test was conducted on the de-seasonalised Rrs to identify significant (99% confidence level) increasing or decreasing trends and a linear regression fitted to estimate the magnitude of the trend.

2.2 Classification models and analysis tools

A bloom threshold of high Rrs was required in order to build classification models for each *Longhurst* [1998] province. The mean Rrs and associated standard deviation (σ) was calculated for each province and the following classes defined: (1) pixels (Rrs > 1σ) classified as 1 (bloom presence); (2) pixels (Rrs=0) classified as 0 (bloom absence); (3) pixels (0 < Rrs ≤ 1σ) were discarded. This resulted in significant class imbalance: in order to build a classifier model, a balanced random forest classifier [e.g., *Khoshgoftaar et al.*, 2007] was used[2] which subsampled from both classes during training. An optimal combination of 500 trees and maximum tree depth of 10 was selected after hyperparameter tuning and testing on a sample of provinces. These hyperparameters were tested on imbalanced and subsample-balanced test sets. Results showed that a low maximum tree depth threshold was necessary to prevent overfitting and improve the prediction of the minority class in the random forest.

A variant of Shapeley Additive exPlanations (SHAP) analysis [*Lundberg and Lee*, 2017], TreeSHAP [*Lundberg et al.*, 2020], was used to explain the contribution of each variable (Table 1 - SST, PAR, MLD, wind speed and stress) to the prediction of Rrs in each *Longhurst* [1998] province. TreeShap utilises the model structure to explicitly model the conditional expected prediction, avoiding breaking the dependencies between correlated variables, as dictated by the rules of causal inference [*Janzing et al.*, 2020]. SHAP values were calculated using the probability of predicting a bloom (from the balanced random forest classifier output) for a sample of 2000 test dataset values, thus balancing computational efficiency with a sufficient sample size. The entire test dataset was used where an individual province contained less than 2000 samples. Finally, to obtain a metric of the relative (ranked) variable importance on determining Rrs from the SHAP values the absolute mean was taken over the sample of explanations for each variable.

3 Results and Discussion

[2] https://imbalanced-learn.org/stable/references/generated/imblearn.ensemble.BalancedRandomForestClassifier.html

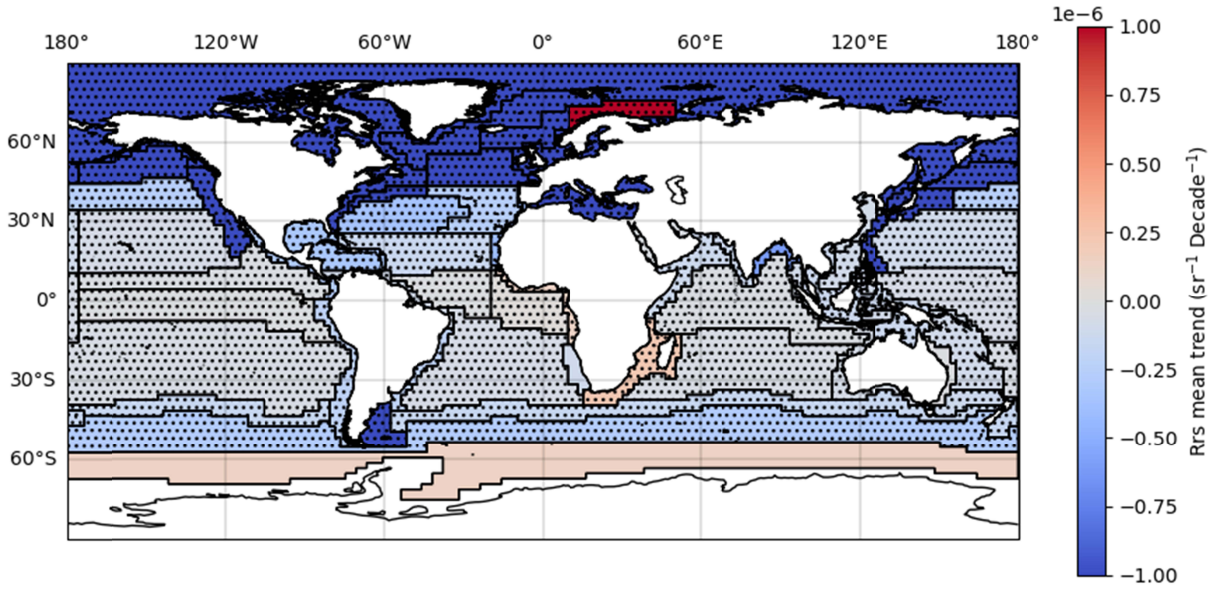

Figure 2. Trends in Rrs for the *Longhurst* [1998] provinces. Stippling indicates significant trend.

Figure 1 shows that the introduction of the sea-ice mask has significantly reduced the surface area affected by high Rrs (by up to 3.8 million km^2), particularly in the Southern Ocean, in comparison to the original decadal analysis [*Loveday and Smyth*, 2018]; this is particularly pronounced around the Antarctic Peninsula. The areas of high Rrs remain consistent with known coccolithophore bloom occurrence: the Barents Sea [*Smyth et al.*, 2004], Bering Sea [*Merico et al.*, 2003], Norwegian Sea [*Andruleit*, 1997], NW European shelf break [*Land et al.*, 2018; *Morozov et al.*, 2013], subarctic North Atlantic [*Raitsos et al.*, 2006], and the Great Calcite belt [*Balch et al.*, 2011] in the Southern Ocean. Globally, there has been an overall downward trend in bloom area of 0.288 million km^2 per decade (Figure S1) with a total loss of 1.15 million km^2 in the past 40 years.

Trends in Rrs for each *Longhurst* [1998] province (Figure 2) show significant decreases (>0.75 µsr^{-1} dec^{-1}) over most of the northern hemisphere, with the notable exception of the Barents Sea (significant increases 6.47 µsr^{-1} dec^{-1}) in marked contrast to the surrounding high latitude seas. In the southern hemisphere, the Antarctic province shows moderate increases (increased magnitude of trend and significance in recent years (1992-2016: Figure S2) as does the East Africa coastal province (0.21 µsr^{-1} dec^{-1}); the Patagonian Shelf, with previously reported blooms [*Signorini et al.*, 2006], shows a marked decrease (1.71 µsr^{-1} dec^{-1}), with a slight decrease in the (0.29 µsr^{-1} dec^{-1}) in the Subantarctic province which includes part of the Great Calcite Belt [*Balch et al.*, 2011]. Tropical regions, generally not associated with coccolithophore blooms, typically have lower trends (less than ±0.20 µsr^{-1} dec^{-1}), and therefore we exclude these from further analysis.

The contrasting trends in the neighbouring Norwegian and Barents Seas warrant further investigation: Figure 3 (a) shows an example month of bloom conditions in the Norwegian Sea and (b) illustrates the ranked SHAP analysis for the entire time-series period. The top 5 drivers of changes to Rrs in rank order are (1) PAR; (2) mean wind speed; (3) MLD; (4) mean wind stress; and; (5) SST with higher values of PAR and SST (high feature value) having a positive

impact on Rrs (positive SHAP value) whereas higher wind speeds, wind stress and greater MLDs are associated with a negative impact on Rrs. This implies that conditions conducive to coccolithophore bloom formation in the Norwegian Sea are dominated by calmer conditions, greater insolation (PAR), a shallower MLD and warmer SSTs. Therefore, reductions in Rrs intensity in the Norwegian Sea (Figure 2) are likely to have been driven by a reduction in PAR, and increases in wind-speed and as a consequence stress and a deepening of the MLD.

For the Barents Sea (Figure 3 (c), (d)), warmer SSTs are the dominant driver of increased Rrs, which is consistent with the local climatic conditions being strongly influenced by the temperature of the inflowing Atlantic water which in turn has a profound effect on ice cover extent, the biology, and coccolithophore succession [*Kogeler and Rey*, 1999]. Intriguingly, increases in PAR are associated with a negative impact on Rrs which is in contrast to the

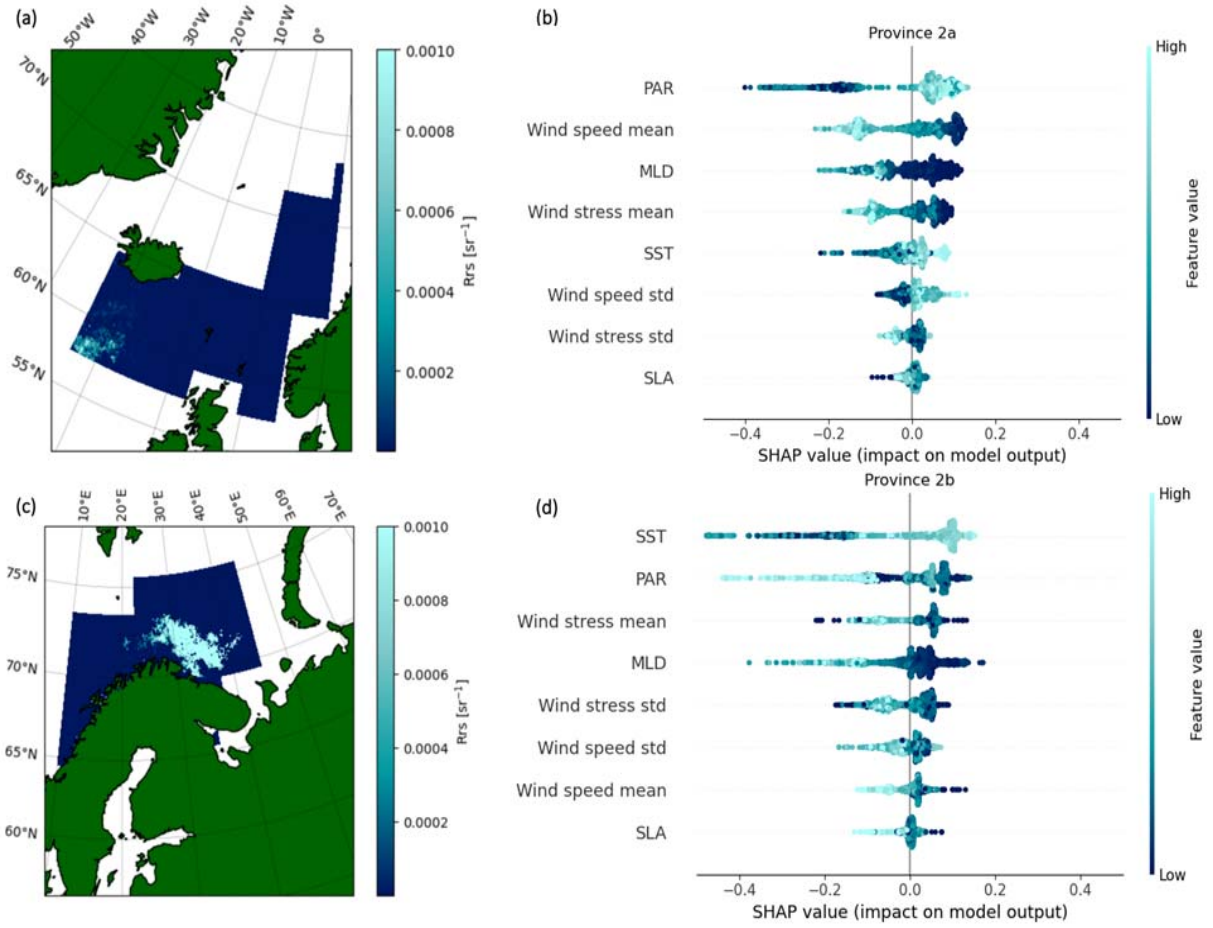

Figure 3. (a) Example bloom conditions of Rrs in the Norwegian Sea (August 2008); (b) SHAP analysis for entire time-series for Norwegian Sea; (c) Example bloom conditions of Rrs in the Barents Sea (August 2008); (d) SHAP analysis for entire time-series for Barents Sea.

Norweigan Sea. As expected a negative impact on Rrs is caused by a deeper MLD (rank 4) and stronger (rank 3, 7) but more variable (rank 5, 6) windspeed and stress. Figure 4 (a) shows that all three provinces (Barents Sea, East Africa coastal, Antarctic, numbered as 2b, 23, 52 respectively) where there are positive trends in Rrs (Figure 2) are primarily driven by changes in SST and secondarily PAR (Figure 4 (b)). However closer inspection reveals fundamental

differences between these provinces: warmer SSTs drive an increase in Rrs in the Barents Sea (2b: Figure 3(d)) but a reduction in Rrs in the East Africa coastal (23: Figure S3(p)) and Antarctic (52: Figure S4(l)) provinces. Intuitively increases in short-wave (PAR) heat flux [*Smyth et al.*, 2014] will tend to warm the surface ocean thereby increasing water column stability, conditions which favour (increasing Rrs) the development of coccolithophore blooms [*Smyth et al.*, 2002; *Tyrrell et al.*, 1999] and *vice versa* (reducing Rrs). For the three provinces where Rrs has been increasing, this intuition only holds true in the Antarctic province (52: Figure S4(l)). In the Barents Sea (2b: Figure 3(d)) and East Africa coastal (23: Figure S3(p)) higher PAR is associated with lower Rrs (absence of blooms). Globally PAR is highly ranked as a driver of reduction in Rrs, being either the primary (Figure 4 (a)) or secondary (Figure 4 (b)) for the majority of provinces.

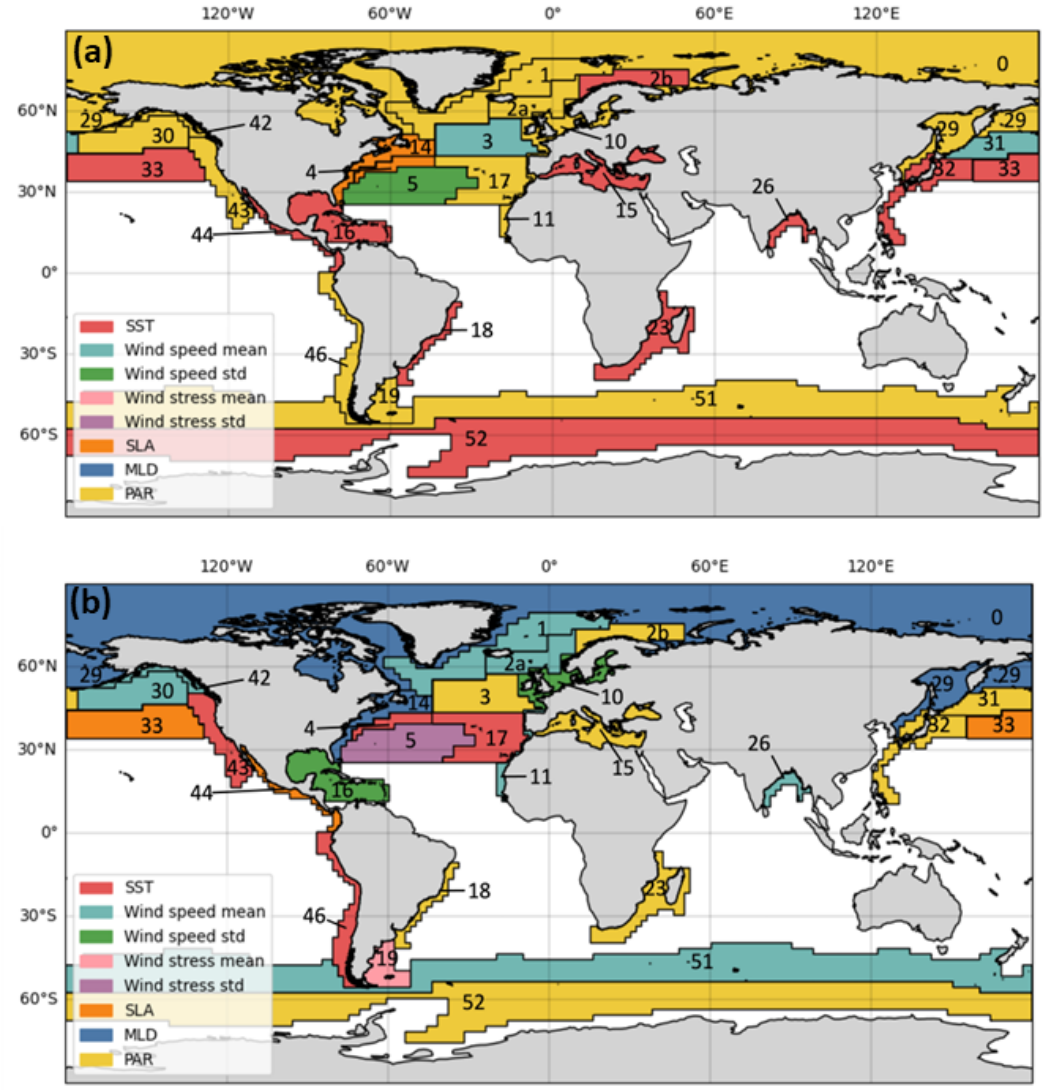

Figure 4. Drivers of Rrs trend by Longhurst [1998] province: (a) Primary driver; (b) Secondary driver.

In the western Atlantic (provinces 4, 5, 14), the dominant drivers (of a reduction in Rrs) appear to be more large-scale dynamical in nature with changes in SLA (province 4, 14), which would point to changes in circulation patterns, and variability in the wind speed (province 5) which could be attributable to an increase in fluctuations between extremes (calm to storm). The supplementary materials contain analyses of the ranked SHAP analyses (Figures S3, S4) in each province together with the associated decadal trends for each of the drivers, (Figures S5, S6).

Figure 1 and Figure S1 show that there has been an overall decrease in bloom area of around 1.15 million km^2 over the past 40 years which is consistent with *Uz et al.* [2013] who attributed this to warmer SST and increasing MLDs. Figure 3 and Figure 4 clearly show that, although SST may be implicated in the poleward movement of coccolithophores in some provinces (even individual seas e.g., Barents Sea), the global picture is more nuanced with multiple drivers acting simultaneously to reduce or increase the likelihood of bloom occurrence (Figures S3, S4).

4 Conclusions

Using a 40-year long, consistently calibrated global dataset of Rrs we have shown an overall decrease in the occurrence of coccolithophores in the global ocean, but marked increases in some high latitude provinces, such as the Barents Sea and the Antarctic Ocean. By using other large datasets of meteorological and oceangraphic parameters over a similar time-period, within a Machine Learning framework, we have shown that those high latitude increases are driven primarily by changes in SST. Decreases elsewhere in the global ocean are driven by other external factors which are specific to individual provinces.

Acknowledgments

ED was supported by The Alan Turing Institute's internship scheme, The Turing Internship Network. DC was funded by the UK National Environment Research Council Earth Observation Data Acquisition and Analysis Service (NEODAAS), grant number NE/S013377/1. TS was funded by the UK Natural Environment Research Council through its National Capability Long-term Single Centre Science Programme, Climate Linked Atlantic Sector Science, grant number NE/R015953/1, and is a contribution to Theme 1.3 – Biological Dynamics. TS was also supported by the Simons Collaboration on Computational Biogeochemical Modeling of Marine Ecosystems/CBIOMES (Grant ID: 549947,SS). Computing resources on the MAssive GPU for Earth Observation (MAGEO) cluster were provided through NEODAAS.

Open Research

The data on which this article is based are available from https://doi.pangaea.de/10.1594/PANGAEA.892175 [*Loveday and Smyth*, 2018]; E.U. Copernicus Marine Service Information (CMEMS). Marine Data Store (MDS). DOIs: 10.48670/moi-00185, 10.48670/moi-00148; https://doi.org/10.21957/pocnex23c6 [*Simmons et al.*, 2006]. The processing and analysis software is available from https://github.com/E-Duncan/coccolithophore_analysis

References

Andruleit, H. (1997), Coccolithophore fluxes in the Norwegian-Greenland Sea: Seasonality and assemblage alterations, *Marine Micropaleontology*, *31*(1-2), 45-64.

Balch, W. M. (2018), The Ecology, Biogeochemistry, and Optical Properties of Coccolithophores, *Annual Review of Marine Science*, *10*(1), 71-98.

Balch, W. M., P. M. Holligan, S. G. Ackleson, and K. J. Voss (1991), Biological and optical properties of mesoscale coccolithophore blooms in the Gulf of Maine, *Limnology and Oceanography*, *36*(4), 629-643.

Balch, W. M., D. T. Drapeau, B. C. Bowler, E. Lyczskowski, E. S. Booth, and D. Alley (2011), The contribution of coccolithophores to the optical and inorganic carbon budgets during the Southern Ocean Gas Exchange Experiment: New evidence in support of the "Great Calcite Belt" hypothesis, *Journal of Geophysical Research: Oceans*, *116*(C4).

Balch, W. M., et al. (2016), Factors regulating the Great Calcite Belt in the Southern Ocean and its biogeochemical significance, *Global Biogeochemical Cycles*, *30*(8), 1124-1144.

Brown, C. W., and J. A. Yoder (1994), Coccolithophorid blooms in the global ocean, *J. Geophys. Res.*, *99*, 7467-7482.

Gordon, H. R., G. C. Boynton, W. M. Balch, S. B. Groom, D. S. Harbour, and T. J. Smyth (2001), Retrieval of coccolithophore calcite concentration from SeaWiFS imagery, *Geophys. Res. Lett.*, *28*, 1587-1590.

Groom, S. B., and P. M. Holligan (1987), Remote Sensing of coccolithophore blooms, *Adv. Space Res.*, *7*, 273-278.

Heidinger, A. K., W. C. Straka, C. C. Molling, J. T. Sullivan, and X. Q. Wu (2010), Deriving an inter-sensor consistent calibration for the AVHRR solar reflectance data record, *Int. J. Remote Sens.*, *31*(24), 6493-6517.

Henson, S. A., D. Raitsos, J. P. Dunne, and A. McQuatters-Gollop (2009), Decadal variability in biogeochemical models: Comparison with a 50-year ocean colour dataset, *Geophysical Research Letters*, *36*, 4.

Iglesias-Rodriguez, M. D., C. W. Brown, S. C. Doney, J. Kleypas, D. Kolber, Z. Kolber, P. K. Hayes, and P. G. Falkowski (2002), Representing key phytoplankton functional groups in ocean carbon cycle models: Coccolithophorids, *Global Biogeochemical Cycles*, *16*, Art 47.

Janzing, D., L. Minorics, and P. Blobaum (2020), Feature relevance quantification in explainable AI: A causal problem, paper presented at 23rd International Conference on Artificial Intelligence and Statistics (AISTATS), Electr Network, Aug 26-28.

Kendall, M. G. (1975), *Rank Correlation Methods*, 4th ed., Charles Griffin, London.

Khoshgoftaar, T. M., M. Golawala, J. Van Hulse, and I. C. Soc (2007), An empirical study of learning from imbalanced data using random forest, paper presented at 19th IEEE International Conference on Tools with Artificial Intelligence, Patras, GREECE, Oct 29-31.

Kogeler, J., and F. Rey (1999), Ocean colour and the spatial and seasonal distribution of phytoplankton in the Barents Sea, *Int. J. Remote Sens.*, *20*(7), 1303-1318.

Land, P. E., J. D. Shutler, and T. J. Smyth (2018), Correction of Sensor Saturation Effects in MODIS Oceanic Particulate Inorganic Carbon, *IEEE Transactions on Geoscience and Remote Sensing*, *56*(3), 1466-1474.

Longhurst, A. (1998), *Ecological geography of the sea*, 398 pp., Academic Press, San Diego.

Loveday, B. R., and T. Smyth (2018), A 40-year global data set of visible-channel remote-sensing reflectances and coccolithophore bloom occurrence derived from the Advanced Very High Resolution Radiometer catalogue, *Earth System Science Data*, *10*(4), 2043-2054.

Lundberg, S. M., and S. I. Lee (2017), A Unified Approach to Interpreting Model Predictions, in *31st Annual Conference on Neural Information Processing Systems (NIPS)*, edited, Long Beach, CA.

Lundberg, S. M., G. Erion, H. Chen, A. DeGrave, J. M. Prutkin, B. Nair, R. Katz, J. Himmelfarb, N. Bansal, and S. I. Lee (2020), From local explanations to global understanding with explainable AI for trees, *Nature Machine Intelligence*, *2*(1), 56-67.

Mann, H. B. (1945), Non-parametric tests against trend, *Econometrica*, *13*, 163 - 171.

Merchant, C. J., et al. (2014), Sea surface temperature datasets for climate applications from Phase 1 of the European Space Agency Climate Change Initiative (SST CCI), *Geoscience Data Journal*, *1*(2), 179-191.

Merico, A., T. Tyrrell, C. W. Brown, S. B. Groom, and P. I. Miller (2003), Analysis of satellite imagery for Emiliana huxleyi blooms in the Bering Sea before 1997, *Geophysical Research Letters*, *30*, Art 1337.

Morozov, E., D. Pozdnyakov, T. Smyth, V. Sychev, and H. Grassl (2013), Space-borne study of seasonal, multi-year, and decadal phytoplankton dynamics in the Bay of Biscay, *Int. J. Remote Sens.*, *34*(4), 1297-1331.

Raitsos, D. E., S. J. Lavender, Y. Pradhan, T. Tyrrell, P. C. Reid, and M. Edwards (2006), Coccolithophore bloom size variation in response to the regional environment of the subarctic North Atlantic, *Limnology and Oceanography*, *51*(5), 2122-2130.

Rost, B., and U. Riebesell (2004), Coccolithophores and the biological pump: responses to environmental changes, in *Coccolithophores: From Molecular Processes to Global Impact*, edited by H. R. Thierstein and J. R. Young, pp. 99-125, Springer Berlin Heidelberg, Berlin, Heidelberg.

Signorini, S. R., V. M. T. Garcia, A. R. Piola, C. A. E. Garcia, M. M. Mata, and C. R. McClain (2006), Seasonal and interannual variability of calcite in the vicinity of the Patagonian shelf break (38°S–52°S), *Geophysical Research Letters*, *33*(16).

Simmons, A., S. Uppala, D. Dee, and S. Kobayashi (2006), ERA-Interim: New ECMWF reanalysis products from 1989 onwards., *ECMWF Newsletter*, *110*, 26 - 35.

Smyth, T. J., T. Tyrrell, and B. Tarrant (2004), Time series of coccolithophore activity in the Barents Sea, from twenty years of satellite imagery, *Geophysical Research Letters*, *31*(11).

Smyth, T. J., G. F. Moore, S. B. Groom, P. E. Land, and T. Tyrrell (2002), Optical modeling and measurements of a coccolithophore bloom, *Applied Optics*, *41*(36), 7679-7688.

Smyth, T. J., I. Allen, A. Atkinson, J. Bruun, R. Harmer, R. Pingree, C. Widdicombe, and P. Somerfield (2014), Ocean Net Heat Flux Influences Seasonal to Interannual Patterns of Plankton Abundance, *PLoS One, doi:10.1371/journal.pone.0098709*.

Tyrrell, T., P. M. Holligan, and C. D. Mobley (1999), Optical impacts of oceanic coccolithophore blooms, *J. Geophys. Res.*, *104*(C2), 3223-3241.
Uz, S. S., C. W. Brown, A. K. Heidinger, T. J. Smyth, and R. Murtugudde (2013), Monitoring a sentinel species from satellites: detecting emiliania huxleyi in 25 years of AVHRR imagery, in *Satellite-based Applications on Climate Change*, edited, pp. 277-288, Springer.
Winter, A., J. Henderiks, L. Beaufort, R. E. M. Rickaby, and C. W. Brown (2013), Poleward expansion of the coccolithophore Emiliania huxleyi, *J. Plankton Res.*, *36*(2), 316-325.